

SUPPLEMENTARY MATERIAL FOR: TECHNO-ECONOMIC AND ENVIRONMENTAL ASSESSMENT OF ETHYL ESTER BIODIESEL

Ediane S. Alves¹, Simone C. Miyoshi², Andrew M. Elias³, Erich Potrich^{4,5}, Letícia P. Miranda¹, Paulo W. Tardioli¹, Roberto C. Giordano¹, Felipe F. Furlan¹

¹Chemical Engineering Program, Federal University of São Carlos (PPGEQ-UFSCar), São Carlos, São Paulo, Brazil.

²Chemical Engineering Program, COPPE, Federal University of Rio de Janeiro (UFRJ), Cidade Universitária, Rio de Janeiro, Brazil.

³Embrapa Instrumentação, Rua XV de Novembro 1452, São Carlos, SP, 13560-970, Brazil.

⁴Department of Renewable Energy Technology (CEAD), Federal University of Piauí (UFPI), Teresina, Piauí, Brazil.

⁵ Graduate Program in Technology, Management and Sustainability (PPGTGS), Federal Institute of Education, Science and Technology of Goiás (IFG), Goiânia, Goiás, Brazil.

Contents

A	NRTL parameters used in the simulation
B	Cogeneration System
C	Operational specifications of CLEA production
D	Operational specifications of equipment modeled in Aspen
E	Construction and results of the Meta-Models
F	Economic assumptions and operating costs
G	CBios calculation according to the RenovaBio Program
H	Life Cycle Assessment of the Free lipase and CLEA immobilization
I	Calorific heat
J	Variable of sensitivity analysis

A - NRTL parameters used in the simulation

Table A.1 presents the of components for biodiesel production.

Table A.1: List of components used in the simulation of biodiesel production.

1	Water
2	Ethanol
3	Glycerol
4	Chloride hydroxide
5	Soybean oil
6	Biodiesel
7	Fatty acids
8	Sodium hydroxide
9	Tert-butanol
10	Oxygen
11	Carbon dioxide
12	Cellulose
13	Enzyme (CLEA)
14	Hemicellulose
15	Lignin

The estimated properties include: normal melting temperature (T_{mp}), normal boiling temperature (T_{bp}), critical temperature (T_c), critical pressure (P_c), critical volume (V_c), acentric factor (ω), standard enthalpy of formation (H_f), standard Gibbs free energy of formation (G_f), vapor phase heat capacity (C_{pv}), liquid heat capacity (C_{pl}), and vapor pressure (P_{vp}). The vapor phase was defined as an ideal gas, while the liquid phase followed the NRTL thermodynamic model. The free fatty acid, soybean oil, and biodiesel were represented as pseudo-components formed by a mixture of free fatty acids, triglycerides, and soybean ethyl ester. The properties of the pseudo-components were consistent with those presented in [1]. The parameters used in the NRTL model are shown in Table A.2. If a component was absent during the liquid-liquid or liquid-vapor equilibrium phases (in the decanter, distillation column, or flash separation), it was assumed to exhibit perfect equilibrium behavior. In this case, its NRTL parameters were set to zero. For example, NaOH was added and subsequently removed, resulting in a mass concentration of less than 1% during the equilibrium steps, leading to $A_{ij} = 0$, $A_{ji} = 0$, $B_{ij} = 0$, $B_{ji} = 0$, and $\alpha = 0$.

Table A.2: NRTL parameters used in simulation to build the meta models.

	Aij	Aij	Bij	Bji	Cij
Biodiesel-Ethanol^a	0.0000	0.0000	567.0400	7054.7000	0.2000
Ethanol -Glycerol^a	0.0000	0.0000	565.7600	16.0600	0.2000
Glycerol- Biodiesel^a	0.0000	0.0000	1004.2000	393.4800	0.2000
Ethanol-Water^b	-0.8009	3.4578	246.1800	-586.0809	0.3000
Glycerol-Water^b	-0.7318	-1.2515	170.9167	272.6075	0.3000
Biodiesel-Water^c	9.2225	6.6520	-2397.7400	617.1190	0.2000
Biodiesel-FFA^d	0.0000	0.0000	-193.8000	-135.0000	0.4445
Soybean oil -Biodiesel^d	0.0000	0.0000	-828.9700	-489.9100	0.1001
Soybean oil -FFA^d	0.0000	0.0000	-26.4300	-181.9900	0.3688

Source: ^a [2];

^b Aspen e VRTherm database;

^c Ardila et al. [3];

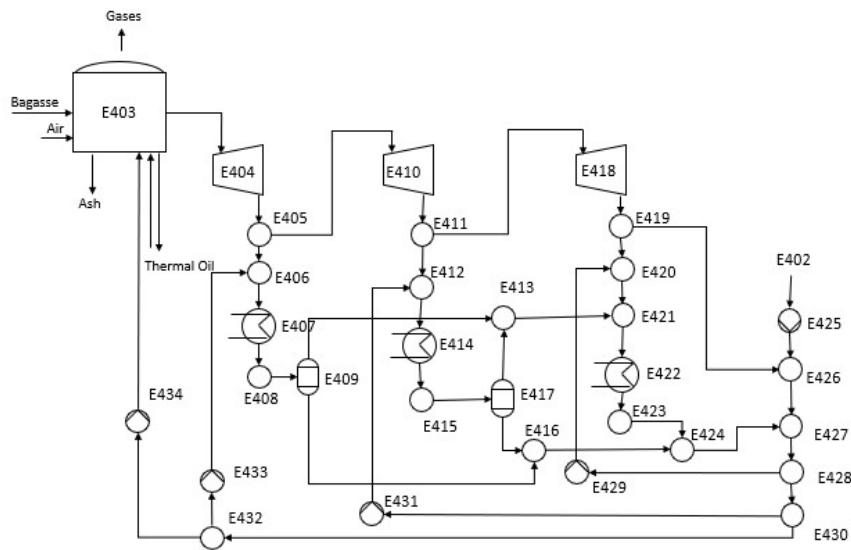
^d Shiozawa et al. [4].

B - Cogeneration System

The boiler was fueled with bagasse and sugarcane straw. It is considered that all combustion reactions are complete, resulting in the production of carbon dioxide and water as byproducts. Figure B.1 illustrates the cogeneration system of the soybean oil and biodiesel biorefinery. To produce biodiesel using alkaline catalysis, the cogeneration system comprises only two turbines for generating medium-pressure steam (10 bar) and low-pressure steam (2.5 bar). However, in all other cogeneration scenarios, there is a need to produce high-pressure steam (41 bar) and to heat thermal oil to meet the heat demand in the reboiler of the distillation column. For brevity, only the process description utilizing three turbines is provided. The boiler and turbines of the soybean biorefinery operate under the same conditions in both simulations.

The boiler operates at 485 °C and 65 bar, with an isentropic efficiency of 80% and mechanical efficiency of 95%. The steam generated in the boiler is directed to turbine E404, which produces steam at 41 bar to meet the demand of the biodiesel column. The turbine E410 generates steam at 10 bar, providing heat for the ethanol dehydration columns and oil extractors. Finally, turbine E418 produces exhaust steam at 2.5 bar, which is utilized to meet various demands across the three processes.

Figure B.1: Soybean biorefinery cogeneration system without condensing turbines.



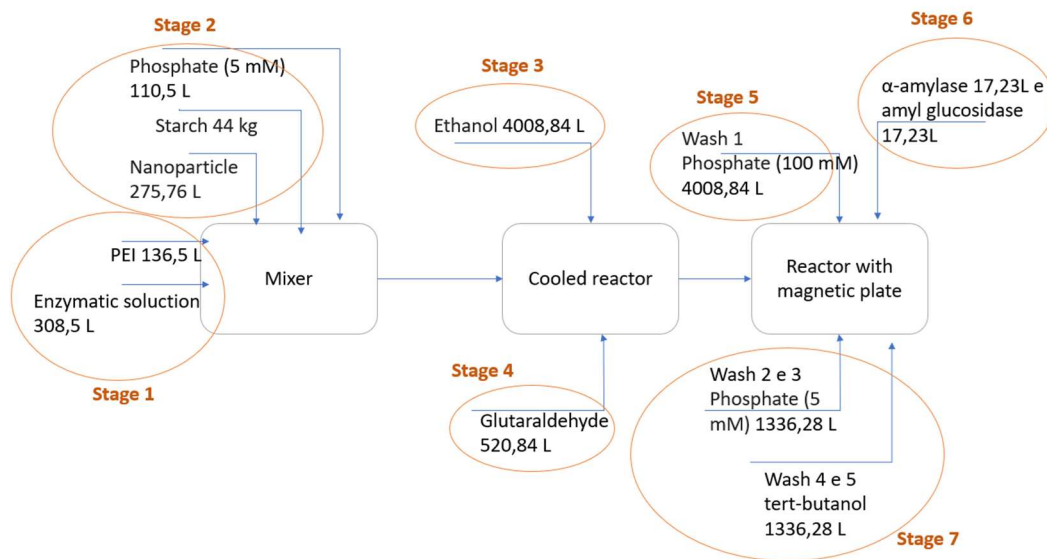
As mentioned earlier, the heat exchangers E407, E414, and E422 are used to calculate the heat demand for each steam line and simulate the pressure losses in the lines, which are assumed to be 4% of the steam passing through the heat exchanger. Water replacement is managed through stream S402. Additionally, the boiler heats thermal oil to meet the demands of the AGL separation column and oil extractors, which operate above 250 °C.

C - Operational specifications of CLEA production

CLEA was produced using a batch process, as illustrated in the block diagram in Figure C.1. The production volume varied according to the biodiesel production stage's demand. The process begins in a rotating tank, where an aqueous solution is prepared containing polyethyleneimine (PEI) at 75 mg/mL, the Eversa Transform (ET) enzyme in a 1:1 mass ratio (mg of protein per mg of PEI), and 5 mM sodium phosphate buffer at pH 7.0. This mixture is stirred for 1 hour at 150 rpm. Next, magnetic silica nanoparticles functionalized with amino and octyl groups (NPMSs) are added in a 1:3 mass ratio (enzyme:NPMSs), along with a solution of soluble starch diluted in phosphate buffer (5 mM, pH 7.0). The resulting enzyme solution is then transferred to a refrigerated rotating drum maintained at 4 °C, where enzyme precipitation occurs upon the addition of ethanol in a 1:3 volume ratio (enzyme:ethanol solution). After 30 minutes, glutaraldehyde is added to the mixture containing the precipitated enzyme, and the solution is stirred at 4 °C and 150 rpm for 2.5 hours to facilitate cross-linking.

The CLEA formed is transferred to a second rotating drum equipped with a magnetic plate, which enables the separation and collection of the immobilized enzyme. The remaining liquid phase is sent to an evaporator, where the ethanol used for enzyme precipitation is recovered. The recovered ethanol is then directed to a distillation column for purification and recycling.

Figure C.1: Simplified process flow diagram for enzyme immobilization in the form of CLEA.



The CLEA retained by the magnetic field in the rotating drum was washed twice with 100 mM sodium phosphate buffer (pH 7.0), using a volume equal to that of ethanol added during the precipitation step, at room temperature. After the washing step, the CLEA was resuspended in 5 mM sodium phosphate buffer (pH 7.0). Subsequently, the enzymes α -amylase (BAN 480L) and amyloglucosidase (AMG 300L) were added to the suspension, and the mixture was incubated at room temperature for 4 hours to promote the hydrolysis of starch into dextrin, maltose, and glucose.

After hydrolysis, the CLEAs were recovered by magnetic separation and subjected to two additional washes with 5 mM sodium phosphate buffer (pH 7.0), followed by two more washes with tert-butanol. The volumes of phosphate buffer and tert-butanol used in these steps were equal to the initial volume of the enzyme solution before the precipitation step. After the final washing, the enzyme catalyst was dried at room temperature. This step was adapted from the method described by Miranda et al. [5], in which drying was conducted at 4 °C. CLEA production batches were initiated every 6 hours, ensuring a continuous supply aligned with the demand of the biodiesel production process.

D - Operational specifications of equipment modeled in Aspen

The equipment simulation using Aspen software, not all components of the operational streams from the main EMSO simulation were included. Only the components present in the equipment were added to the Aspen simulation. The operational specifications for the simulation are presented in Table D.1.

Table D.1: Range of variables used in the construction of the kriging meta-model and the correlation coefficients of the outputs from the modeled equipment.

Decanter	
Parameter	Value
Decanter temperature	40.0 °C

Hydrated ethanol column	
Parameter	Value
Number of stages	47.0
Feed stages	23.0
Top pressure	116.0 kPa
Bottom pressure	135.7 kPa
Purity of hydrated ethanol	93.5 % (in mass)

Tert-Butanol A1 column	
Parameter	Value
Number of stages	27.0
Feed stages	22.0
Supply pressure	0.3 atm
Column pressure	0.3 atm
Column temperature	45.2 °C
Purity of tert-butanol	99.0% (in mass)

Tert-Butanol A2 column	
Parameter	Value
Number of stages	6.0
Feed stages	3.0
Column pressure	0.2 atm
Purity of glycerol	99.0% (in mass)

Biodiesel column	
Parameter	Value
Number of stages	25.0
Feed stages	6.0
Column pressure	1.4 kPa
Purity of biodiesel	98.0 % (in mass)

Free fatty acid column	
Parameter	Value
Number of stages	60.0
Feed stages	12.0
Column pressure	35.0 kPa
Purity of biodiesel	95.0 % (in mass)

In the decanter simulation, only the temperature and feed mass fraction were specified, while the calculation of the thermodynamic equilibrium for phase separation determined the output conditions. Liquid-liquid equilibrium data were specific to the equilibrium of biodiesel, ethanol, water, and glycerol. It was assumed that the fatty acids and soybean oil behave similarly to biodiesel. In this simulation, biodiesel was represented by ethyl linoleate ester, which constitutes 50 - 60% of the biodiesel formed by the transesterification of soybean oil [6]. For biodiesel and free fatty acid distillation column, the components included biodiesel (represented by ethyl linoleate), linolenic acid (representing all the free fatty acids in the process, and trilinolein (representing soybean oil). Other components comprised less than 0.2 % of the mixture. The distillation column for producing hydrated ethanol follows the configuration described by Dias et al. [7] and Furlan et al. [8]. The distillation of tert-butanol was simulated as proposed by Lo and Chien [9], with some adaptations. The glycerol extractive distillation column used for anhydrous alcohol purification to return to the reaction employs a mathematical interpolation developed by Potrich et al. [1].

E - Construction and results of the Meta-Models

A Universal Kriging model was used to represent the equilibrium equipment simulations performed in Aspen and the soybean oil extraction process. From the outputs of the meta-model, it was possible to calculate the total mass balance, mass balance per component, and the energy balance, thereby determining the flow of the equipment output streams. The output and input variables of the meta-model are summarized in Table E.1. The range of the input variables for the mass fraction in the distillation columns were determined by varying the column feed composition, reflecting different conversions of the esterification and transesterification reactions across four scenarios. The temperature was adjusted by changing the working temperature by a few degrees to provide flexibility in the process. For the decanter input variables, the maximum and minimum values were based on the experimental data used to calculate the thermodynamic data for the liquid-liquid balance

of the decantation system. The variation of the oil extraction meta-model input was conducted randomly, with the midpoint of the variation range corresponding to the value used in the simulation.

Table E.1: Range of variables used in the construction of the kriging meta-model and the correlation coefficient of the outputs of the modeled equipment.

Decanter				
Variables	Lower bounds	upper bounds	Correlation coefficient (r ²)	Mean square error(mse)
Mass Fraction ethanol	0.060	0.200	-	-
Mass Fraction Biodiesel	0.610	0.870	-	-
Mass Fraction Glycerol	0.010	0.170	-	-
Glycerol percentage ^a	-	-	0.997	9.758 E-3
Ethanol percentage ^a	-	-	0.995	7.424 E-3
Water percentage ^a	-	-	0.994	7.215 E-3
Biodiesel percentage ^a	-	-	0.992	4.708 E-3
Ethanol Distillation Column				
Variables	Lower bounds	upper bounds	Correlation coefficient (r ²)	Mean square error(mse)
Temperature	100 °C	130 °C	-	-
Mass Fraction ethanol	0.570	0.860	-	-
Mass Fraction water	0.140	0.430	-	-
Water ethanol ^a	-	-	0.999	5.456 E-4
Water percentage ^a	-	-	0.999	2.888 E-5
Reboiler heat	-	-	0.999	1.800 E-4
Condenser heat	-	-	0.999	1.181 E-2
Tert-butanol Distillation Column				
Variables	Lower bounds	upper bounds	Correlation coefficient (r ²)	Mean square error(mse)
Temperature	25° C	40 °C	-	-
Mass Fraction Butanol	0.900	0.970	-	-
Mass Fraction water	0.030	0.100	-	-
Tert-butanol percentage ^a	-	-	0.998	8.482 E-5
Water percentage ^a	-	-	0.996	1.137 E-3
Reboiler 01 heat	-	-	0.998	1.691 E-5
Condenser 01 heat	-	-	0.966	2.599 E-2
Reboiler 02 heat	-	-	0.985	1.018 E-3
Condenser 02 heat	-	-	0.956	4.058 E-2
Biodiesel Distillation Column				
Variables	Lower bounds	upper bounds	Correlation coefficient (r ²)	Mean square error(mse)
Temperature	100 °C	130 °C	-	-
Mass Fraction Soybean oil	0.034	0.110	-	-
Mass Fraction Fatty Acid	0.015	0.061	-	-
Biodiesel percentage ^a	-	-	0.982	2.142 E-4
Fatty Acid percentage ^a	-	-	0.985	3.240 E-3
Reboiler heat	-	-	0.977	8.067 E-4
Condenser heat	-	-	0.980	4.072 E-1

Fatty Acid Distillation Column				
Variables	Lower bounds	upper bounds	Correlation coefficient (r ²)	Mean square error(mse)
Mass Fraction Biodiesel	0.110	0.190	-	-
Mass Fraction Fatty Acid	0.110	0.480	-	-
Mass Fraction Soybean Oil	0.350	0.760	-	-
Biodiesel percentage ^a	-	-	0.996	3.666 E-4
Fatty Acid percentage ^a	-	-	0.998	3.895 E-4
Reboiler heat	-	-	0.998	1.631 E-2
Condenser heat	-	-	0.999	4.664 E-4
Oil Extraction				
Variables	Lower bounds	upper bounds	Correlation coefficient (r ²)	Mean square error(mse)
Soybean oil mass flow	90	130	-	-
Fraction Breaker	0.057	0.076	-	-
Conditioner Temperature	328 °C	338 °C	-	-
Expander Temperature	388 °C	398 °C	-	-
Extractor yield	0.966	0.986	-	-
Evaporator 01 Concentration	0.560	0.760	-	-
Evaporator 02 Concentration	0.950	0.970	-	-
Degummed soybean oil production	-	-	0.999	3.740 E-10
Refine soybean oil production	-	-	0.999	3.920 E-10
Meal production	-	-	0.999	2.950 E-10
Lecithin production	-	-	0.999	4.910 E-10
Hull production	-	-	0.999	3.080 E-10
Energy consumption	-	-	0.999	9.353 E-20
Low pressure consumption	-	-	0.999	1.260 E-05
Medium pressure consumption (degummed oil process)	-	-	0.999	1.650 E-05
Medium pressure consumption (refine oil process)	-	-	0.999	1.650E-05
Cold utility consumption	-	-	0.999	6.020 E-10
Hexane consumption	-	-	0.999	4.180 E-10
Water consumption	-	-	0.999	1.260 E-05

^a The output variables of the meta-model were the percentages of the mass flow of the feed directed to the output streams. For example, if 100 kg/h of alcohol were fed into the decanter and 80 kg/h of alcohol were fed directed to the glycerol-rich phase, the meta-model output for alcohol would be 0.8. This indicates that 80% of the ethanol was directed to the glycerol-rich phase, while 20% was sent to the biodiesel-rich phase.

Table E.2 presents the number of points used in the construction of the meta-models.

Table E.2: Number of points used in the construction of meta-models.

Meta-model	Number of points for construction
Decanter	600
Ethanol distillation column	100
tert-butanol distillation column	80
Biodiesel distillation column	110
AGL distillation column	100
Soybean oil extraction	1000

F – Economic assumptions and operating costs

Operational costs for soybean oil degumming and biodiesel production derived from the economic assumptions outlined is table F.1.

F.1: Economic assumptions for the analysis.

Economic assumptions	Value	Reference
Minimum attractive rate of return (annual)	11%	Longati et al. [10]
Plant lifetime	25 years	Longati et al. [10]
Tax rate (income and social contributions)	34%	Longati et al. [10]
Depreciation rate (linear, 10 years)	10%	Peters et al. [11]
Residual value of the plant	Zero	Peters et al. [11]
Exchange rate	4.995 BRL	Cepea USP [12]
Contingence cost	5% of Total Plant Cost	Peters et al. [11]
Working capital	10% of CAPEX	Peters et al. [11]
Indirect costs	32.5% of Total Direct Cost	Peters et al. [11]
Project construction time	2 years	Assumed
Plant scrap value	Zero	Assumed
Hours worked in a year	8 048.22 h	Assumed
Cold utility cost	4.85 USD/MW h	Peters et al. [11]
Refrigeration cost	0.185 USD/t	Turton et al. [13]
Operating labor	15% of operation cost	Peters et al. [11]
Operating supervision	10% of operating labor	Peters et al. [11]
Maintenance	4% of Total Fixed Capital	Peters et al. [11]
Operating supplies	10% of Maintenance Cost	Peters et al. [11]
Laboratory charges	10% of Operating Labor	Peters et al. [11]
Patent royalty	1% of Direct Production Costs	Peters et al. [11]
Plant overhead	1% of operating labor and Operating Supervision	Peters et al. [11]
Administrative	20% of operating Labor and Operating Supervision	Peters et al. [11]
Research Development	Zero	Peters et al. [11]
Distribution and Marketing	Zero	Peters et al. [11]

Table F.2 outlines the average input costs and product prices over the last five years for the process studied. The dataset is specific to the Brazilian context.

F.2: Average price of products and raw materials over the last five years.

Economic assumptions	Value	Reference
Alfa-amylase enzyme	6630.67 USD/m ³	Comex [15]
Amyloglucosidase enzyme	26829.76 USD/m ³	Comex [15]
Anhydrous ethanol	510.30 USD/t	Cepea USP [12]
Biodiesel	705.56 USD/t	ANP [17]
Blond glycerol	318.03 USD/t	Comex [15]
CBio BRL	69.75 BRL/CBio	Observatório da cana[19]
CBio USD	13.96 USD/CBio	Observatório da cana[19]
Electricity	35.64 USD/MW	CCEE [18]
Eversa® Transform 2.0 enzyme	15000.00 USD/t	Andrade et al. [16]
Free fatty acid	1402.11 USD/t	Comex [15]
Glutaraldehyde	3457.96 USD/t	Comex [15]
Glycerol	711.41USD/t	Comex [15]
Hexane	805.92 USD/t	Comex [15]
Hydrochloric acid (HCl)	1883.72 USD/t	Comex [15]
Hydrous ethanol	458.25 USD/t	Cepea USP [12]
Lecithin	1026.78 USD/t	Comex [15]
Magnetic nanoparticles	30000.00 USD/m ³	Personal Communication
Polyethyleneimine	6825.94 USD/t	Comex [15]
Sodium hydroxide (NaOH)	652.94 USD/t	Comex [15]
Sodium Phosphate	2082.87 USD/t	Comex [15]
Soybean	432.66 USD/t	Comex [15]
Soybean hulls	396.54 USD/t	Comex [15]
Soybean meal	441.04 USD/t	Comex [15]
Soybean oil	1275.04 USD/t	Comex [15]
Starch	458.12 USD/t	Comex [15]
Sugarcane bagasse	20.02 USD/t	Personal Communication
tert-Butanol	1268.25 USD/t	Comex [15]
Waste oil ^a	406.06 USD/t	Personal Communication
Water	4.35 USD/m ³	Cedae [14]

^a The cost of waste oil includes the collection costs, which are based on 6 m³ collection vehicles travelling an average distance of 30 km

The operating costs for oil extraction were determined using the assumptions and data specified in the extraction sector simulation (see Table F.3).

Table F.2: Variable cost of soybean oil extraction. Source: [1].

Solvent preparation, extraction and recovery	
Labor	USD 2.2733/t processed soybean
Maintenance and service	USD 2.7147/t processed soybean
Cold Utilities	USD 0.0014/t processed soybean
Other costs	USD 0.3053/t processed soybean

G – CBios calculation according to the RenovaBio Program

The carbon intensity of the biofuel, measured in ton CO_{2eq}, is calculated according to Matsuura et al. [20] and is subtracted from that of its fossil fuel equivalent. One Cbio is equivalent to 1 ton of CO_{2eq} of avoided emission. For example, ethanol is compared to gasoline (87.4 g CO_{2eq}/MJ), and biodiesel to diesel (86.5 g CO_{2eq}/MJ). The resulting difference represents the potential for greenhouse gas (GHG) reduction per MJ of fuel consumed in vehicles. This value generates the Energy-Environmental Efficiency Rating, which, when combined with the volume of biofuel produced, is converted into CBio, as shown in equation G.1.

$$C_{bio} = \left\{ Fossil.fuelx \left(\frac{CO_{2eq}}{Mj} \right) - Biodieselx \left(\frac{CO_{2eq}}{Mj} \right) \right\} x Biodiesel.production(Mj) \quad (G.1)$$

H - Life Cycle Assessment of the Free lipase and CLEA immobilization

The LCA inputs were based on the study by Raman et al. [21], with the exception of the use of soybean oil and protein, which replaced palm oil and corn protein to better adapt the process to the Brazilian context. The scope of the LCA study was from cradle to gate, and the GWP 100 was calculated using the AR5 of the IPCC (2014):

The determination of inputs and outputs of the enzyme immobilization process, the data were derived from the simulation described in Section C of the Supplementary Material. The impact caused by the tert-butanol solvent, even when used to wash the CLEA before initiating a new batch of biodiesel production, was allocated to the production of the CLEA, as the solvent was fully recovered in the same column. In contrast, the impact

caused by ethanol, including that used in the precipitation of the enzyme, was allocated to the production of biodiesel due to the joint recovery process. The life cycle assessment of lipase and CLEA production is shown in Table H.1. For the immobilization enzyme, certain approximations were also made for the components. Polyethyleneimine was represented by ethylamine. Given the higher contribution of glutaraldehyde in the inventory, we opted to conduct a Life Cycle Assessment (LCA) based on the methodology of Sanders et al. [22]. The production process of glutaraldehyde was simulated using Aspen to construct the inventory. One of the main components in glutaraldehyde production is ethyl vinyl ether, for which an LCA was also calculated for global warming potential based on Sixt [23]. The inventories and impacts of both glutaraldehyde and ethyl vinyl ether are presented in Table H.2, where mass allocation for the compounds was applied. For the enzymes α -amylase and amyloglucosidase, the inventory was based on data available in the U.S. Life Cycle Inventory Database (USLCI) [24], specifically for Alpha-amylase (Novozyme Liquozyme/kg/RER) and Glucoamylase (Novozyme Spirizyme/kg/RER). The inventories and impacts of both enzymes are detailed in Table H.3. The impacts used to construct the LCA for this study are presented in Table H.4.

Table H.1: LCA of GWP Emissions for Free and Immobilized Lipase in Generic Production

Description	Unit	Free lipase production		Description	Unit	CLEA immobilization	
		Input Unit/ kg enzyme	g CO _{2eq.}			Input Unit/ kg CLEA	g CO _{2eq.}
<i>Inputs</i>				<i>Inputs</i>			
Water	kg	26.450	0.233	Eversa® Transform 2.0	kg	2.765	6286.102
Ammoniums sulfate	kg	0.251	323.816	Polyethyleneimine	kg	0.009	16.853
Magnesium sulfate	kg	0.025	26.026	<i>Phosphate</i>	kg	1.073	2992.652
Starch from Soybean (Glucose)	kg	0.754	976.214	Magnetic nanoparticles	kg	3.596	34.809
Soy protein	kg	0.476	119.938	Glutaraldehyde	kg	5.399	16676.126
Soy Oil	kg	1.382	769.691	α -amylase	kg	0.002	3.487
Energy	kW	0.286	57.537	Amyloglucosidase	kg	0.002	14.103
Total	kg	1.000	2273.455	Starch	kg	0.001	0.486
			2273.455	Tertbutanol	kg	0.000	0.319
				Colling	MJ	8.150	553.071
				Total	kg	1.000	26578.009

Table H.2: LCA of GWP Emissions for Glutaraldehyde (GLU) and Ethyl Vinyl Ether (EVE) Production.

Description	Unit	Glutaraldehyde (GLU) production		Description	Unit	Ethyl vinyl ether (EVE) production	
		Input Unit/ kg GLU	g CO _{2eq.}			Input Unit/ kg EVE	g CO _{2eq.}
<i>Inputs</i>				<i>Inputs</i>			
Acrolein	kg	0.583	1449.770	vinyl acetate	kg	2.656	6129.278
Vinyl ethyl ether	kg	0.750	2715.019	Ethanol	kg	0.719	344.396
Water	kg	0.180	0.002	Mercury acetate ^a	kg	0.023	0.000
Energy	kW	1.716	345.242	Sulfuric acid	kg	0.000	0.043
Total	kg	1.000	4510.032	Energy	kW	1.560	313.839
				Total	kg	1.000	6787.555
<i>Outputs</i>				<i>Outputs</i>			
Ethanol	kg	0.460	1421.288	Vinyl ethyl ether	kg	1.000	3620.030
Glutaraldehyde	kg	1.000	3088.745	Acetic acid	kg	0.875	3167.526

a- The contribution of this component was disregarded due to the low value in the inventory.

Table H.3: LCA of GWP Emissions for α -amylase and amyloglucosidase production

Description	Unit	Alfa-Amylase (α -Amy) production		Description	Unit	Amyloglucosidase (AMG) production	
		Input Unit/ kg α -Amy	g CO _{2eq.}			Input Unit/ kg AMG	g CO _{2eq.}
Inputs				Inputs			
Energy, from coal	Mj	65.700	3671.513	Energy, from coal	Mj	14.000	782.362
Water	m ³	0.029	5.757	Water	m ³	0.012	2.382
Transformation, from pasture, man made	m ²	1.000	26.098	Transformation, from pasture, man made	m ²	0.300	7.829
Transformation, to industrial area	m ²	1.000	26.098	Transformation, to industrial area	m ²	0.300	7.829
Emissions				Emissions			
Carbon dioxide, emissions to air	kg	4.400	4400.000	Carbon dioxide, emissions to air	kg	1.200	1200.000
Sulfur dioxide, emissions to air ^a	kg	0.000	0.000	Sulfur dioxide, emissions to air ^a	kg	0.000	0.000
Ethene, emissions to air ^a	kg	0.000	0.000	Ethene, emissions to air ^a	kg	0.000	0.000
Phosphate, emissions to soil ^b	kg	0.000	0.000	Phosphate, emissions to soil ^b	kg	0.000	0.000
Outputs				Outputs			
Alpha-amylase	kg	1.000	8129.467	Amyloglucosidase	kg	1.000	2000.403

a- The contribution of this component was disregarded due to the low value in the inventory;

b- The output does not contribute to the GWP 100 impact category.

Table H.4: GWP 100 data used.

Item	Unit	Kg CO_{2eq}	Data Base	Description
Acrolein	kg	2.486	IPCC (2014) [25] Ecoinvent 3.8	market for acrolein acrolein Cutoff, U - GLO
Ammoniums sulfate	kg	1.290	IPCC(2014) [25] Ecoinvent 3.8	market for ammonium sulfate ammonium sulfate Cutoff, U - Row
Carbon dioxide, emissions to air	kg	1.000	IPCC (2014) [25] Ecoinvent 3.8	
CO _{2eq} from bagasse burning	kg	0.006	IPCC (2006) [26]	
Colling	kg	0.068	IPCC (2014) [25] Ecoinvent 3.8	
Cooling water*	MJ	0.154	RenovaCalc [20]	
Effluent treatment	kg	1.599E-4	RenovaCalc [20]	
Energy	MJ	0.056	IPCC (2014) [25] Ecoinvent 3.8	electricity, high voltage, production mix electricity, high voltage Cutoff, U - BR
Ethanol	kg	0.479	Potrich et al. [1]	
HCl	kg	1.676	RenovaCalc [20]	
Hexane	kg	0.309	Potrich et al. [1]	
Magnesium sulfate	kg	1.041	IPCC(2014) [25]Ecoinvent 3.8	market for magnesium sulfate magnesium sulfate Cutoff, U - GLO
Magnetic nanoparticles	kg	0.010	Feijoo et al. [27]	PEI coated magnetite NPs
NaOH	kg	0.513	RenovaCalc [20]	
Phosphate	kg	2.789	IPCC(2014) [25]. Ecoinvent 3.8	sodium phosphate production sodium phosphate Cutoff, U - RoW
Polyethyleneimine	kg	1.873	IPCC(2014) [25]. Ecoinvent 3.8	market for polyester-complexed starch biopolymer polyester-complexed starch biopolymer Cutoff, U - GLO
Road Transport 60m ³	km	0.032	RenovaCalc [20]	
Soybean	kg	0.308	RenovaCalc [20]	
Soybean Oil	kg	0.557	Potrich et al. [1]	
Soybean protein	kg	0.252	Potrich et al. [1]	
Starch	kg	0.830	IPCC (2014) [25] Ecoinvent 3.8	market for maize starch maize starch Cutoff, U - GLO

Starch from Soybean (Glucose)	kg	1.295	IPCC(2014) [25] Ecoinvent 3.8	market for glucose glucose Cutoff, U - GLO
Sulfuric acid	kg	0.109	RenovaCalc [20]	
Tert-butanol	kg	2.833	IPCC (2014) [25] Ecoinvent 3.8	market for 2-methyl-2-butanol 2-methyl-2-butanol Cutoff, U - GLO
Transformation, from pasture, man made	ha	261.000	IPCC (2014) [25] Ecoinvent 3.8	land use change, pasture, man made land use change, pasture, man made Cutoff, U - BR
Transformation, to industrial area	ha	261.000	IPCC (2014) [25] Ecoinvent 3.8	land use change, pasture, man made land use change, pasture, man made Cutoff, U - BR
Vinyl acetate	kg	2.307	IPCC (2014) [25] Ecoinvent 3.8	market for vinyl acetate vinyl acetate Cutoff, U - GLO
Water	kg	8.80E-6	RenovaCalc [20]	
Water, cooling, unspecified	kg	1.985E-4	IPCC (2014) [25] Ecoinvent 3.8	tap water production, conventional treatment tap water Cutoff, U - BR

*Heat removed from water 1.61E-4 MJ/kg

I - Calorific heat

Table I.1: Calorific value of components.

Item	Unit	Value
Soybean oil ^a	MJ/kg	34.04
Soybean meal ^a	MJ/kg	15.40
Lecithin ^a	MJ/kg	31.90
Soybean hull ^a	MJ/kg	15.10
Anhydrous ethanol ^a	MJ/kg	28.26
Hydrated ethanol ^a	MJ/kg	26.38
Biodiesel (B100) ^a	MJ/kg	37.68
Free fatty acid ^b	MJ/kg	38.26

Source: a – Matsuura et al. [20];

b – Pawar et al. [28];

J – Variable of sensitivity analysis

J.1: Variables subjected to sensitivity analysis and their ranges of variation.

Variable	DFT/WET		DIT	
	Min	Max	Min	Max
Oil/ethanol molar ratio	1:4	1:6	1:4	1:6
Enzyme Price (USD)/kg	6.4	15	6.4	15
Reaction time (hours)	4	12	4	12
Reaction Temperature (K)	303	328	303	328
Biodiesel yield after Transesterification (Conversion efficiency)	0.856	0.951	0.856	0.951
Hydrolysis conversion	0.012	0.034	0.012	0.034
Enzyme Reuse	4	12	5	50

References

- [1] E. Potrich, S.C. Miyoshi, P.F.S. Machado, F.F. Furlan, M.P.A. Ribeiro, P.W. Tardioli, R.L.C. Giordano, A.J.G. Cruz, R.C. Giordano, J. Clean. Prod. 244 (2020) 118660. <https://doi.org/10.1016/j.jclepro.2019.118660>.
- [2] F.M.R. Mesquita, F.X. Feitosa, N.E. Sombra, R.S. Santiago-Aguiar, H.B. Sant'Ana, J. Chem. Eng. Data 56 (2011) 4061-4067. <https://doi.org/10.1021/je200340x>.
- [3] Y.C. Ardila, A.B. Machado, G.M.F. Pinto, R.M. Filho, M.R.W. Maciel, J. Chem. Eng. Data 58 (2013) 605-610. <https://doi.org/10.1021/je301028r>.

- [4] S. Shiozawa, D. Gonçalves, M.C. Ferreira, A.J.A. Meirelles, E.A.C. Batista, *Fluid Phase Equilib.* 507 (2020) 112431. <https://doi.org/10.1016/j.fluid.2019.112431>.
- [5] L.P. Miranda, J.R. Guimarães, R.C. Giordano, R. Fernandez-Lafuente, P.W. Tardioli, *Catalysts* 10 (2020) 817. <https://doi.org/10.3390/catal10080817>.
- [6] H. Omidvarborna, A. Kumar, D.-S. Kim, P.K.P. Venkata, V.S.P. Bollineni, J. Hazard. Toxic Radioact. Waste 19 (2015) 04014030. [https://doi.org/10.1061/\(ASCE\)HZ.2153-5515.0000237](https://doi.org/10.1061/(ASCE)HZ.2153-5515.0000237).
- [7] M. Dias, (2008) [Master's Thesis, Universidade Estadual de Campinas]. Biblioteca Virtual - FAPESP. <https://bv.fapesp.br/en/dissertacoes-teses/74380/simulation-of-ethanol-production-processes-from-sugar-and-su>
- [8] F.F. Furlan, C.B.B. Costa, A.R. Secchi, J.M. Woodley, R.C. Giordano, *Ind. Eng. Chem. Res.* 55 (2016) 9865-9872. <https://doi.org/10.1021/acs.iecr.6b01757>
- [9] K.M. Lo, I.L. Chien, *J. Taiwan Inst. Chem. Eng.* 73 (2017) 27-36. <https://doi.org/10.1016/j.jtice.2016.07.040>.
- [10] A.A. Longati, A.R.A. Lino, R.C. Giordano, F.F. Furlan, A.J.G. Cruz, *Bioresour. Technol.* 263 (2018) 1-9. <https://doi.org/10.1016/j.biortech.2018.04.102>.
- [11] M.S. Peters, K.D. Timmerhaus, R.E. West, *Plant Design and Economics for Chemical Engineers*, 5^ª ed., McGraw-Hill, New York (2003), p. 123.
- [12] Cepea USP, Ethanol price, <https://www.cepea.esalq.usp.br/br/indicador/etanol.aspx> [accessed June 15, 2024].
- [13] R. Turton, R.C. Bailie, W.B. Whiting, J.A. Shaeiwitz, D. Bhattacharyya, *Analysis, Synthesis, and Design of Chemical Processes*, 4^ª ed., Prentice Hall, New Jersey (2012), p. 123.
- [14] CEDEA, Companhia Estadual de Águas e Esgotos do Rio de Janeiro, <https://cedae.com.br/acedae>. [accessed October 8, 2024].
- [15] Comex Stat, General Data, <http://comexstat.mdic.gov.br/pt/geral> [accessed August 26, 2024].
- [16] T.A. Andrade, M. Errico, K.V. Christensen, *Chem. Eng. Trans.* 74 (2019) 769-774. <https://doi.org/10.3303/CET1974129>.
- [17] ANP, Biodiesel Auctions, <https://www.gov.br/anp/pt-br/assuntos/distribuicao-e-revenda/leiloes-biodiesel> [accessed June 15, 2024].
- [18] CCEE, Settlement Price of Differences, <https://www.ccee.org.br/> [accessed June 15, 2024].
- [19] Observatório da Cana, <https://unicadata.com.br/listagem.php?idMn=110>. [accessed September 12, 2024].
- [20] M.I.S.F. Matsuura, M.T. Scachetti, M.F. Chagas, J.E.A. Seabra, M.M.R. Moreira, A.M. Bonomi, G. Bayma, J.F. Picoli, M.A.B. Morandi, N.P. Ramos, O. Cavalett, R.M.L. Novaes, Método e Ferramenta para a Contabilidade da Intensidade de Carbono de Biocombustíveis no Programa RenovaBio, <https://www.gov.br/anp/pt-br/assuntos/consultas-e-audiencias->

publicas/consulta-audiencia-publica/2018/arquivos-consultas-e-audiencias-publicas-2018/cap-10-2018/cp10-2018_nota-tecnica-renova-calc.pdf. [accessed January 26, 2022].

- [21] J.K. Raman, V.F.W. Ting, R. Pogaku, Biomass Bioenergy 35 (2011) 4221-4229.
<https://doi.org/10.1016/j.biombioe.2011.07.010>.
- [22] H.J. Sanders, G. Walker, H. Edwards, T. Hall, Ind. Eng. Chem. 50 (1958) 854-860.
<https://doi.org/10.1021/ie50582a021>.
- [23] J. Sixt, Methods for producing vinyl ethers, UY, 2984688 (1961).
- [24] USLCL, National Renewable Energy Laboratory, <https://www.nrel.gov/analysis/lci.html>. Published 2024. [accessed February 8, 2024].
- [25] IPCC, Climate Change 2007 Synthesis Report,
https://www.ipcc.ch/site/assets/uploads/2018/02/ar4_syr_full_report.pdf [accessed January 16, 2023].
- [26] IPCC, Guidelines for National Greenhouse Gas Inventories, Intergovernmental Panel on Climate Change (2006). <https://www.ipcc-nggip.iges.or.jp/public/2006gl/vol1.html> [accessed October 10, 2024].
- [27] S. Feijoo, S. González-García, Y. Moldes-Diz, C. Vazquez-Vazquez, G. Feijoo, M.T. Moreira, J. Clean. Prod. 143 (2017) 528-538. <https://doi.org/10.1016/j.jclepro.2016.12.079>.
- [28] S. Pawar, J. Hole, M. Bankar, S. Khan, S. Wankhade, Mater. Today Proc. (2023).
<https://doi.org/10.1016/j.matpr.2023.01.375>.